

Photoinduced One-Electron Oxidation of Benzyl Methyl Sulfides in Acetonitrile. Time-Resolved Spectroscopic Evidence for a Thionium Ion Intermediate

Marta Bettoni,[§] Tiziana Del Giacco,^{*,†‡} Marina Stradiotto,[†] Fausto Elisei^{†‡}

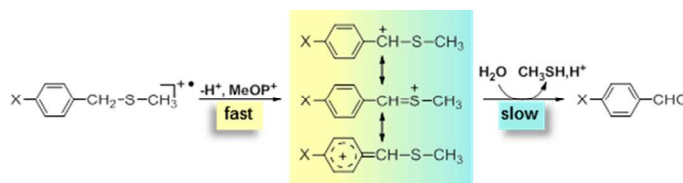
[†]Dipartimento di Chimica, Biologia e Biotecnologie, Università di Perugia, Via Elce di Sotto 8, 06123 Perugia, Italy

[‡]Centro di Eccellenza Materiali Innovativi Nanostrutturati (CEMIN), Università di Perugia, Via Elce di Sotto 8, 06123 Perugia, Italy

[§]Dipartimento di Ingegneria Civile ed Ambientale, Università di Perugia, Via G. Duranti 93, 06125 Perugia, Italy

Email: tiziana.delgiacco@unipg.it

RECEIVED DATE (to be automatically inserted after your manuscript is accepted if required according to the journal that you are submitting your paper to)



ABSTRACT: The photooxidation of 4-methoxybenzyl methyl sulfide (**1a**), benzyl methyl sulfide (**1b**) and 4-cyanobenzyl methyl sulfide (**1c**) has been investigated in the presence of N-methoxy phenanthridinium hexafluorophosphate ($\text{MeOP}^+\text{PF}_6^-$) under nitrogen in CH_3CN . The steady state

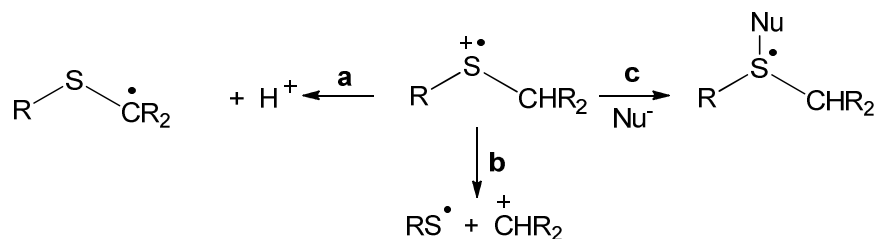
1
2
3 photolysis experiments showed for the investigated sulfides exclusively the formation of the
4
5 corresponding benzaldehyde as oxidation product, reasonably due to a deprotonation of the sulfide
6
7 radical cations. Photooxidation of **1a-1c** occurs through an electron transfer process. Indeed, laser flash
8
9 photolysis measurements showed an efficient formation of sulfide radical cations, detected in their
10
11 dimeric form $[(4\text{-X-C}_6\text{H}_4\text{CH}_2\text{SCH}_3)_2^{+\bullet}]$ at ca. 520 nm. At longer delay times, the absorption of the
12
13 dimer radical cation was replaced by an absorption band assigned to (α -thio)benzyl cation (thionium
14
15 ion, $\lambda_{\text{max}} = 420\text{-}400$ nm), formed by oxidation of the benzyl radical, and not by that of the (α -
16
17 thiomethyl)benzyl radical, as expected if a $\text{C}_\alpha\text{-H}$ bond cleavage is operative. This finding highlights a
18
19 particular stability of this kind of cation never reported before, even though its involvement in one-
20
21 electron oxidation mechanisms of various sulfides has already been invoked. DFT calculations allowed
22
23 to identify a significant charge and spin delocalization involving both the phenyl ring and the sulfur
24
25 atom of the radical cations.
26
27
28
29
30
31
32
33

34 Introduction

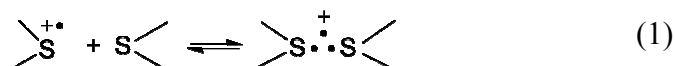
35
36 Organic sulfur radical cations are important intermediates in a great variety of chemical processes,
37
38 extending from those of industrial importance to the synthetic and biological ones.¹ Most studies have
39
40 been carried out on the main reaction pathways of dialkyl sulfide radical cations, only more recently
41
42 radical cations from aromatic sulfides (aryl sulfides having general formula ArSR) have attracted
43
44 considerable attention.² These intermediates, investigated after generation by photoinduced electron
45
46 transfer, radiolysis or chemical and electrochemical oxidation of sulfides, can decay through
47
48 competitive pathways whose relative rate constants depend strongly on the structure of the substrate
49
50 and the experimental conditions (solvent polarity, additives, etc.). Generally, sulfide radical cations
51
52 undergo the most common deprotonation reaction, that involves the cleavage of a C-H bond in β
53
54 position with respect to the sulfur atom (center of positive charge), together with the breaking of the C-
55
56
57
58
59
60

S bond (α -cleavage), which leads to the formation of a sulfenyl radical and a carbocation (Scheme 1, path **a** and **b**, respectively). Moreover, these intermediates can be attached at the sulfur by nucleophilic species (Scheme 1, path **c**), as oxygen and superoxide anion to form sulfoxides.³

Scheme 1



In particular, nucleophiles such as sulfides, can quickly attack sulfur radical cations forming dimeric three-electron bonded complexes (two bonding σ - and one antibonding σ^* -electrons), which are known to establish an equilibrium with the molecular radical cation as formulated in eq. 1.



Asmus et al. have reported numerous examples which substantiated, by experimental data and theoretical considerations, that the radical cations of aliphatic sulfides are stabilized by the formation of a sulfur-sulfur three-electron bond.⁴ Sawaki et al. have argued the formation of dimers also from aromatic sulfides (with a sulfur atom bound to an aromatic ring).⁵ They have investigated radical cations of thioanisoles by laser flash photolysis and reported that both the σ - and π -type dimers are formed depending on the structure and concentration. More recent studies have further confirmed these results.^{2h,,3d,6}

Along this line, we have considered worthwhile to extend these investigations to the one-electron photooxidation of benzyl methyl sulfides **1a-1c**, with different substituents in *para* position on the ring,

by $\text{MeOP}^+\text{PF}_6^-$ in CH_3CN under nitrogen. These reactions have been studied by nanosecond laser flash photolysis (LFP) and steady-state photolysis. The transient species produced, their decay pathways, and the final photoproducts have been identified. The results of this study, reported herewith, have been integrated by DFT calculations, in order to get information on the geometry of the radical cations and, more importantly, the charge and spin distribution. This information was considered to be of great utility to better understand on the dynamics of the radical cation fragmentation process and, in particular, on the SOMO position.

Results

Steady-State Photolysis. Steady state photolysis experiments were carried out by irradiating at 355 nm a N_2 -saturated CH_3CN solution of sulfides **1a-1c** in the presence of $\text{MeOP}^+\text{PF}_6^-$. As already reported,⁷ in these experimental conditions the singlet excited state of N-methoxyphenanthridinium was produced, which undergoes breaking of the N-O bond forming the phenanthridinium radical cation ($\text{P}^{+\bullet}$). This species is a quite powerful oxidant (the estimated reduction potential is 2.0 V vs SCE in CH_3CN)^{7a} able to accept one electron from the investigated sulfides because they have lower oxidation potentials (Table 1), thus forming the corresponding sulfide radical cations (Scheme 2), highlighted by LFP studies.

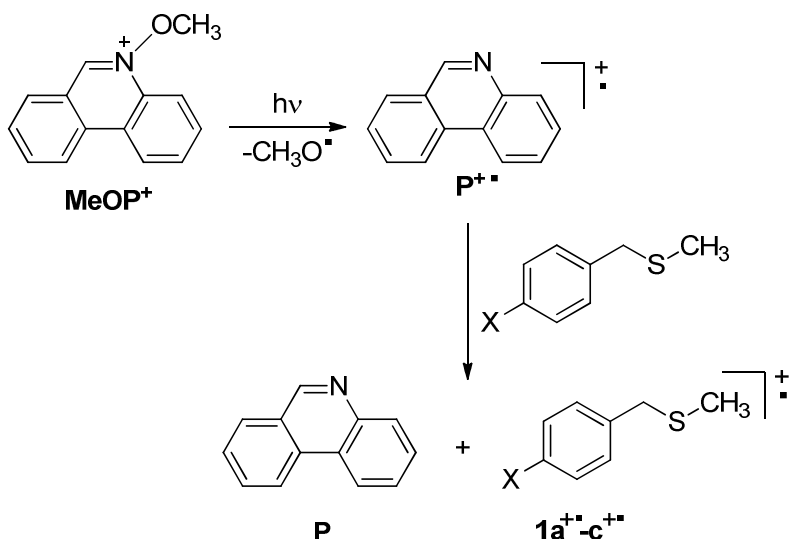
The photolysis of sulfides **1a-1c** produced benzaldehydes (**2a-c**) as only product (Scheme 3).⁸ The products were identified with ^1H -NMR and GC-MS techniques by comparison with authentic specimens.

Table 1. Chemical Yields (%) of the Photoproducts, Relative Rate (k_X/k_H) and Oxidation Potentials (E_p), for the MeOP⁺-Sensitized Photooxidation Reaction of Benzyl Methyl Sulfides **1a–**1c** in N₂-Saturated CH₃CN**

sulfide	unreacted sulfide, ^a (%)	X-C ₆ H ₄ CHO, ^a (%)	k_X/k_H ^b	E_p , ^c V
1a (X=OCH ₃)	77	17	2.25	1.55
1b (X=H)	83	16	1	1.63
1c (X=CF ₃)	88	12	0.47	1.73

^a [Sulfide] = 1.0×10^{-2} M, [MeOP⁺PF₆[−]] = 5.0×10^{-3} M. Yields are referred to the initial amount of substrate. ^b Determined by kinetic competitive experiments (GC analysis of unreacted substrates); [Sulfide] = 5.0×10^{-3} M, [MeOP⁺PF₆[−]] = 5.0×10^{-3} M. ^c Oxidation peak potential vs SCE measured by cyclic voltammetry in air-equilibrated CH₃CN; sweep rate 100 mVs^{−1}.

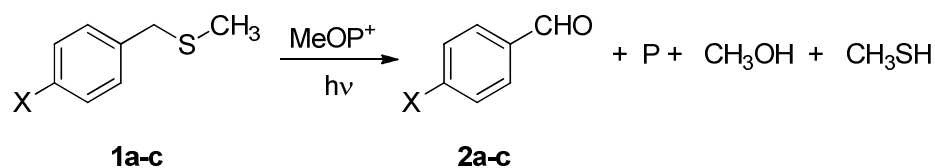
Scheme 2



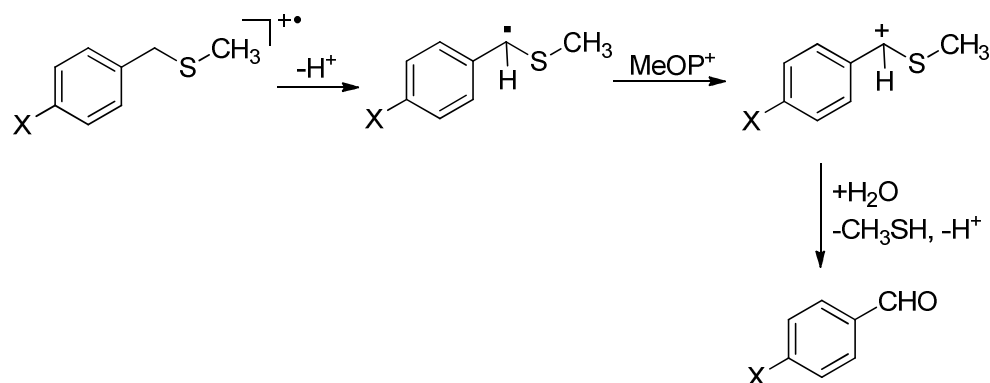
Quantitative analysis, performed by GC using the internal standard method, showed a similar amount of benzaldehyde for each sulfide (17, 16 and 12% for **1a**, **1b** and **1c**, respectively) after 15 min of irradiation (Table 1). The material balance was satisfactory (>94%) in all experiments.

The structure of photoproducts formed can reasonably be rationalized on the basis of the formation of the radical cation followed by benzylic deprotonation (Scheme 4), as already suggested by Albini et al.⁹ for the oxidation of analogous ethyl sulfides (PhCH₂SCH₂CH₃) photosensitized by 9,10-dicyanoanthracene (DCA) and 2,4,6-triphenylpyrylium tetrafluoroborate (TPP⁺BF₄[−]).

Scheme 3



Scheme 4



The resulting (α -thiomethyl)benzyl radical ($4\text{-XC}_6\text{H}_4\text{-CH}^\bullet\text{SCH}_3$) is then oxidized, likely by the ground-state N-methoxyphenanthridinium (vide infra), to the corresponding cation, which forms the final product (benzaldehyde) by reaction with adventitious water. The disappearance of N-methoxyphenanthridinium was checked by recording the UV-visible absorption spectra before and after irradiation; this analysis endorsed the consumption of two $\text{MeOP}^+\text{PF}_6^-$ molecules for each molecule of sulfide. The sulfur-containing product CH_3SH was not identified experimentally because of its high volatility. Other detected products were those deriving from the N-O fragmentation of MeOP^+ (phenanthridine, P, and methanol).

The relative reaction rates, expressed as ratio of the photooxidation rate constant of 4-X- $\text{C}_6\text{H}_4\text{CH}_2\text{SCH}_3$ (k_X) and that of the unsubstituted sulfide (k_H), were determined by the kinetic competitive method (Table 1). As shown in Figure S1 (see Supporting Information), $\log(k_X/k_H)$ values decrease linearly as the sulfide oxidation potential (E_p , Table 1) increases; this result is in line with a

rate-determining electron transfer step from the benzyl methyl sulfide to the phenanthridinium radical cation (Scheme 2). The slope of -0.16 mol/kcal is characteristic of a substrate-like transition state in a slightly exergonic electron-transfer.¹⁰

Laser Flash Photolysis Studies. Upon laser excitation ($\lambda_{\text{exc}} = 355 \text{ nm}$) of N_2 -saturated CH_3CN solutions of sulfides **1a-1c** ($1.0 \times 10^{-2} \text{ M}$) and MeOP^+ ($1.4 \times 10^{-4} \text{ M}$), a broad and intense absorption with maximum around 520 nm was detected just after the laser pulse. As an example, the time resolved spectra of the **1b**/ MeOP^+ system are reported in Figure 1, while those of **1a** and **1c** are shown in Figures S2 and S3 (Supporting Information). Then it seems to be reasonable the attribution of this absorption to the three-electron bonded dimer radical cations, $[(\text{ArCH}_2\text{CH}_3)\text{S} \cdot \cdot \text{S}(\text{ArCH}_2\text{CH}_3)]^+$ -type, formed according to eq. 1. Indeed the corresponding $[(\text{CH}_3)_2\text{S} \cdot \cdot \text{S}(\text{CH}_3)_2]^+$ structure, having a hydrogen atom in place of the aryl group, is reported to absorb at shorter wavelength (465 nm in aqueous solution)¹¹ but it is known that the electron induction, as could be that exerted by the aryl group, into the three-electron ($2\sigma, \sigma^*$) bond can affect the energy of the $\sigma \rightarrow \sigma^*$ transition, which will result in a decrease in bond strength and then to a red shift in the absorption spectrum.^{4b} The absorption bands of the molecular radical cations **1a⁺-1c⁺**, produced by fast oxidation of sulfides **1a-1c** due to the phenanthridine radical cation, which should be in rapid equilibrium with the dimer radical cations, should be around 300 nm,¹² an undetectable spectral position with our experimental set-up. The decay rates of the dimer radical cations, thus corresponding to those of monomer radical cation **1a⁺-1c⁺**,^{5,6a} were determined in the presence of nitrogen by following the kinetics at 600 nm. This wavelength, higher than that corresponding to the λ_{max} , was chosen in order to reduce the overlap of the dimer absorption with that of other transients (vide infra). In all cases, the decay kinetics followed clean first

order laws, in accordance with a unimolecular fragmentation process. The lifetimes (τ) measured at 25°C are reported in Table 2.

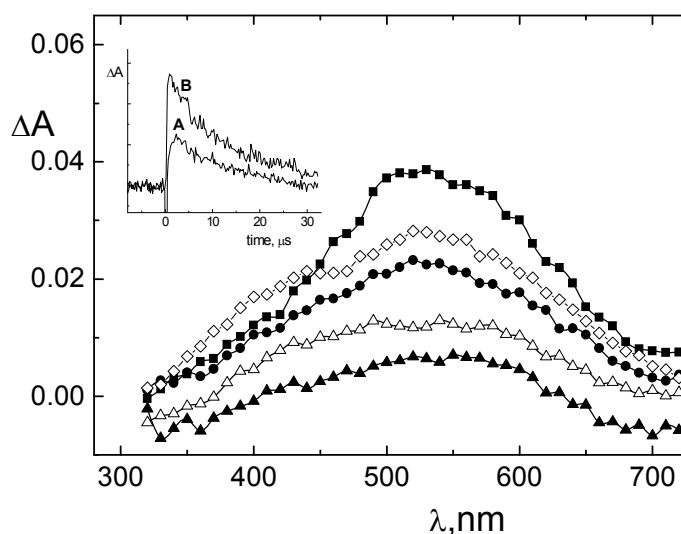


Figure 1. Time-resolved absorption spectra of the MeOP⁺ (1.4×10^{-4} M)/**1b** (1.0×10^{-2} M) system in N₂-saturated CH₃CN recorded 0.88 (■), 2.5 (◇), 7.4 (●), 18 (△) and 32 (▲) μs after the laser pulse. λ_{exc} = 355 nm. Inset: decay kinetics recorded at 400 (A) and 530 (B) nm.

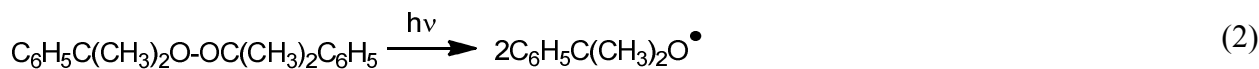
Table 2. Lifetimes of the Dimer Radical Cations Determined without (τ) and with the presence of NO₃[−] Base (τ_{base}), and of the Cations (τ_{C}) Formed in the MeOP⁺-Sensitized Photooxidation Reaction of Benzyl Methyl Sulfides **1a-1c in N₂-Saturated CH₃CN^a**

sulfide	[(ArCH ₂ ,CH ₃)S : S(ArCH ₂ ,CH ₃)] ⁺		4-X-C ₆ H ₄ CHSCH ₃
	τ	τ_{base}^b	τ_{C}
1a (X=OCH ₃)	7.8	0.84	9.8
1b (X=H)	7.7	0.92	16
1c (X=CF ₃)	7.3	0.91	12

^a Values in μs. Experimental error of 10%. ^b [Bu₄N⁺NO₃[−]] = 2.0×10^{-2} M.

The time-evolution of the absorption spectra showed a slow decay of the ΔA signal at 520-550 nm (see insets of Figure 1 and of Figures S2-S3) followed by the growth of the absorption in the 400-450

nm region. The assignment of the absorbance at 400-450 nm to the (α -thiomethyl)benzyl radical formed by deprotonation of the radical cations (Scheme 4) can be excluded on the basis of the following considerations. Firstly, the time-resolved spectra in the 400-450 nm region (see Figure S4) were not influenced by oxygen, that rules out the uncharged nature of the transients. In addition, the absorption maximum for this kind of radicals is expected at shorter wavelengths.¹² Actually, the experimental absorption spectra of $\text{C}_6\text{H}_5\text{CH}^\bullet\text{SCH}_3$ radical was obtained by photolysis of the dicumyl peroxide/**1b** system in CH_3CN , which produced the absorption spectra shown in Figure S5. As already reported,¹³ irradiation of dicumyl peroxide with UV light promotes the formation of cumyloxyl radical $[\text{C}_6\text{H}_5\text{C}(\text{CH}_3)_2\text{O}^\bullet]$ within the laser pulse (eq 2) which displays a broad band at 490 nm. The time-evolution of the absorption spectra shows that this signal decay ($t_{1/2} = 0.6 \mu\text{s}$) is coupled with the growth of the absorption at 340 nm ($t_{1/2} = 0.4 \mu\text{s}$) that can be reasonably attributed to the formation of $\text{C}_6\text{H}_5\text{CH}^\bullet\text{SCH}_3$ (eq 3).¹⁴



On the other hand, on addition of NO_3^- base (as tetra-*n*-butylammonium salt, TBAN, $2.0 \times 10^{-2} \text{ M}$), the lifetimes of the cation radicals $\mathbf{1a}^{+\bullet}$ - $\mathbf{c}^{+\bullet}$ were significantly shortened, as expected. In fact the decay rates of the radical cation dimers, recorded in the presence of TBAN at higher wavelengths (580-600 nm) than λ_{max} (in order to reduce the overlap of these transients with that absorbing at 400 nm), followed clean first-order kinetics (see insets C of Figure 2 and Figures S6 and S7) with lifetime values (see Table 2) about an order of magnitude lower than those obtained in the absence of NO_3^- . According

to these results there is a poor effect of the sulfide structure on the deprotonation rate of the radical cation dimers.

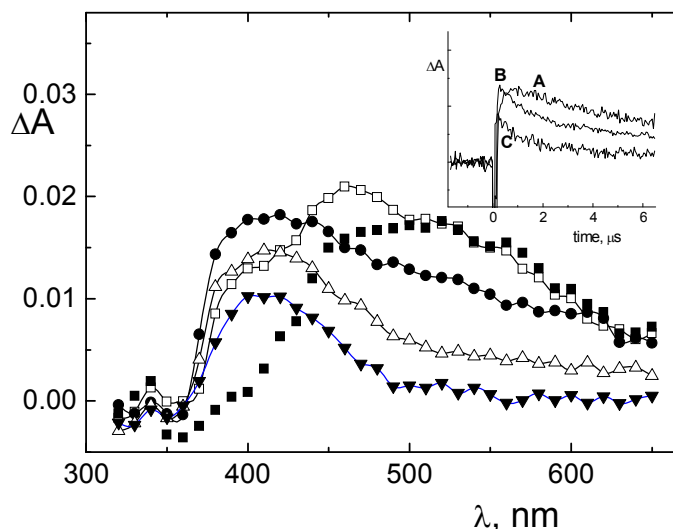


Figure 2. Time-resolved absorption spectra of the MeOP^+ (2.4×10^{-4} M)/**1b** (1.0×10^{-2} M) system in the presence of 2.0×10^{-2} M TBAN recorded 0.18 (■), 0.22 (□), 1.8 (●), 3.0 (△) and 6.4 (▼) μs after the laser pulse in N_2 -saturated CH_3CN . $\lambda_{\text{exc}} = 355$ nm. Inset: decay kinetics recorded at 400 (A), 450 (B) and 580 (C) nm.

As observed, in the presence of NO_3^- , the radical cations generated a transient fully developed at about 0.7, 1.8 and 2.7 μs after the flash with λ_{max} at 420, 410 and 400 nm for **1a**, **1b** and **1c**, respectively. The absorption spectra recorded just after the laser pulse appear as negative signal until ca. 450 nm owing to the bleaching of the $\text{MeOP}^+\text{PF}_6^-$ ground state. From the insets it can be observed that the decay of the radical cations at $\lambda = 580$ nm for **1b** $^{\bullet+}$ (inset C of Figure 2) and at 600 nm for **1a** $^{\bullet+}$ and **1c** $^{\bullet+}$ (insets C of Figures S6 and S7, respectively) is practically synchronous with the buildup of the transient at 400-420 nm (insets A of the corresponding Figures). The effect of NO_3^- can be understood in terms of this anion acting as a Brönsted base with respect to the radical cation, endorsing the hypothesis of the deprotonation as main reaction of the radical cation, responsible of the aldehyde formation (Scheme 4). These results leads us to attribute the bands centered around 400-420 nm to the

(α -thio)benzyl cations, $4\text{-X-C}_6\text{H}_4\text{CH}^+\text{SCH}_3$, obtained by oxidation of the corresponding (α -thio)benzyl radicals, formed by $\text{C}_\alpha\text{-H}$ cleavage of the radical cations. On the other hand, the bathochromic shift of the cation absorption bands of about 80 nm compared to that of the corresponding radicals is in line with what has already been observed with similar species.¹⁶

The kinetic decay recorded at 420 nm is not modified by the presence of oxygen, thus confirming the cationic nature of the transients (in Figure S8 the oxygen effect on the decay rate recorded at 420 nm is shown for **1a** taken as an example). The missing evidence of $4\text{-X-C}_6\text{H}_4\text{C}^\bullet\text{HSCH}_3$ in the time-resolved spectra suggests that rate of its formation is slower than that of its disappearance. This aspect will be discussed in the Discussion Section. The decay kinetics recorded at 400-410 nm were well fitted by first order laws (lifetime values are collected in Table 2). The decay rate should be due to the reaction of the cation with the residual water present in CH_3CN to produce the only product observed by us in steady-state photolysis, $4\text{-XC}_6\text{H}_4\text{CHO}$ (Scheme 4). Indeed the lifetimes did not increase by addition of water, probably because the amount of water in our medium (ca. 2×10^{-2} M) is sufficiently high to trap completely the cation.¹⁷

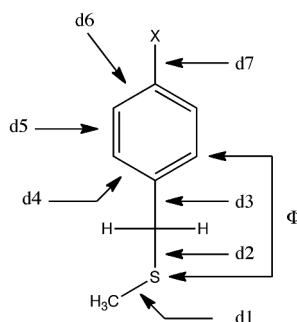


Figure 3. Definition of geometrical features of radical cations **1a**^{•+}-**1c**^{•+} reported in Table 3.

Table 3. Most Significant Dihedral Angle (deg) and Bond Lengths (Å) of Radical Cations $1a^{+\bullet}$ - $1c^{+\bullet}$ in AcN (CPCM model) Optimised by B3LYP/6-311G(d,p)

	Φ	d1	d2	d3	d4	d5	d6	d7
$1a^{+\bullet}$	81	1.820	1.849	1.489	1.416	1.370	1.425	1.321
$1b^{+\bullet}$	82	1.811	1.839	1.500	1.411	1.383	1.405	1.083
$1c^{+\bullet}$	78	1.804	1.836	1.505	1.406	1.383	1.404	1.508

Quantum-mechanical Calculations. Sulfide Radical Cations.

The most significant geometrical features (dihedral angles and bond length as defined in Figure 3) of radical cations $1a^{+\bullet}$ - $1c^{+\bullet}$ are reported in Table 3. From these data it can be observed that the conformations for the radical cations have very similar geometries. In all of the energy minimum conformations the CH_2 -S bond is almost perpendicular to the phenyl ring (the dihedral angle Φ is around 80°). The conformer at the minimum of energy of $1b^{+\bullet}$ is shown in Figure 4 ($1a^{+\bullet}$ and $1c^{+\bullet}$ conformers are reported in Figure S9 in Supporting Information).

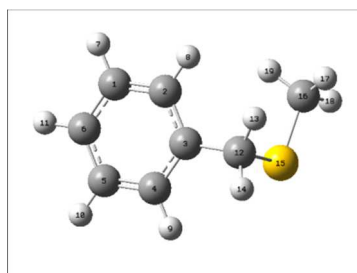


Figure 4. Conformer at the minimum of energy of $C_6H_5CH_2SCH_3^{+\bullet}$ ($1b^{+\bullet}$).

Table 4. NPA Charges (q_{NPA}) and Mulliken Spin Densities for the Most Stable Conformers of Radical Cations $1\mathbf{a}^{+\bullet}$ - $1\mathbf{c}^{+\bullet}$

		X	C ₆ H ₄	CH ₂	S	CH ₃
$1\mathbf{a}^{+\bullet}$ (X=OCH ₃)	q_{NPA}	0.042	0.538	0.064	0.265	0.089
	spin	0.140	0.511	-0.019	0.361	0.007
$1\mathbf{b}^{+\bullet}$ (X=H)	q_{NPA}		0.311	0.097	0.450	0.141
	spin		0.369	0.017	0.640	-0.025
$1\mathbf{c}^{+\bullet}$ (X=CF ₃)	q_{NPA}	0.110	0.103	0.098	0.524	0.165
	spin	0.002	0.243	-0.019	0.749	0.025

The atomic charges were obtained by natural population analysis (NPA).¹⁸ Unpaired electron spin densities were calculated using the Mulliken population analysis. From the NPA charges and spin density data obtained for radical cations $1\mathbf{a}^{+\bullet}$ - $1\mathbf{c}^{+\bullet}$ and reported in Table 4, it can be noted that the charge and spin density of the radical cation are mainly localized on the Ar ring and sulfur. In particular, charge and spin density increase significantly on the sulfur atom (from 0.265 to 0.524 and from 0.361 to 0.749, respectively) at the expense of that on the Ar ring (from 0.538 to 0.103 and from 0.511 to 0.243, respectively) on going from the radical cation $1\mathbf{a}^{+\bullet}$ to $1\mathbf{c}^{+\bullet}$. A reasonable explanation of this distribution is that in the radical cation a through-space interaction between the aromatic ring and the sulfur p orbital takes place, favored from the conformational geometry. This specific interaction is well visualized in the SOMO-2 representation for $1\mathbf{b}^{+\bullet}$ shown in Figure 5 ($1\mathbf{a}^{+\bullet}$ and $1\mathbf{c}^{+\bullet}$ conformers are reported in Figure S10 in Supporting Information). The distribution of charge and spin between the ring and sulfur can also be represented as a contribution of the resonance structures I and II to the conformation of the radical cation (Scheme 5). Obviously, the higher the electron donating power of

the X substituent, the more the resonance structure II contributes to the resonance, as evidenced from the data of Table 4.¹⁹

Some hyperconjugative interaction could be supposed between the C_α-S bond and the π system of the aromatic ring, which can be represented by a contribution of structure III (Scheme 5). The very low charge on the CH₂ group (Table 4) suggests, however, that structure III should be a much less important contributor to the resonance hybrid of the radical cation conformations.

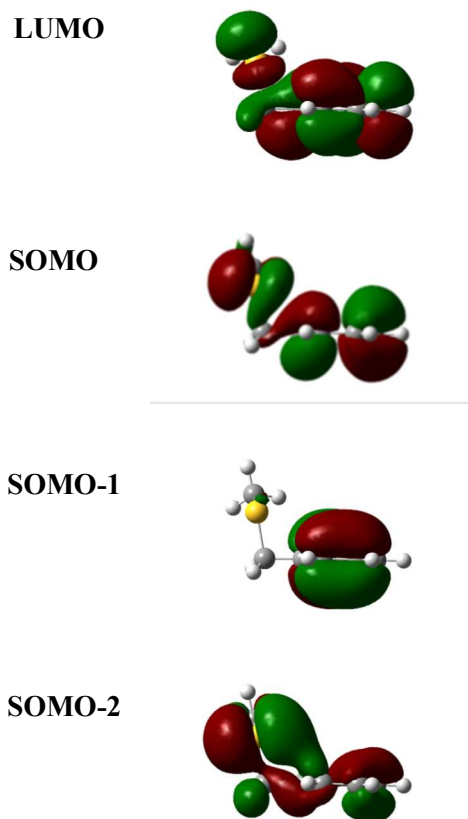
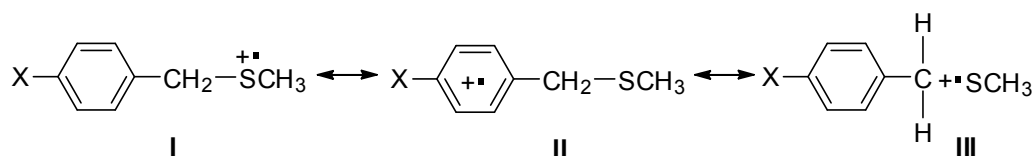


Figure 5. Molecular orbitals of the energy minimum conformer of C₆H₅CH₂SCH₃^{+•} (**1b**^{+•}).

Scheme 5



Discussion

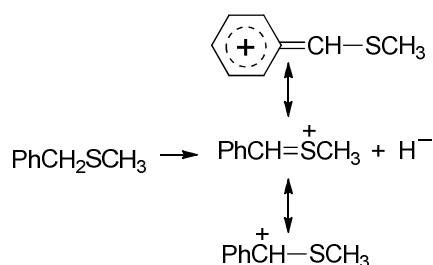
The results of the steady-state photolysis experiments have clearly indicated that in all cases benzaldehydes are formed as the major primary reaction products. The carbonyl compounds are supposed to come from oxidation followed by reaction with adventitious water of the (α -thiomethyl)benzyl carbon radical, which is formed by C_{α} -H bond cleavage in the radical cation (Scheme 4), the intermediate detected by laser flash photolysis experiments within the laser pulse. The possibility of cleavage of the C_{α} -S bond (to give a benzyl cation and a methylthiyl radical) of **1a⁺**-**1c⁺**, together with the deprotonation from the benzylic position, as observed with benzyl phenyl sulfide radical cations,^{3d-e,22} can be experimentally excluded. This is in line with a deprotonation reaction much more exergonic than the C_{α} -S bond cleavage.²³

Peculiarity of this study has been to point out, by flash photolysis experiments, that the intermediate cation (4-X-C₆H₄CH⁺SCH₃), and not its precursor (4-XC₆H₄-CH[•]SCH₃), is accumulated in the **1a-1c** photooxidation. In fact, Asmus et al. observed, by pulse radiolysis investigation, RSR(-H)[•] radical as intermediate in the oxidation of dimethylsulfide and its derivatives by hydroxyl radical, formed by deprotonation of ether monomer radical cation or of the dimer in equilibrium with it (eq 1).^{4a,f} This radical, probably present as hybrid of mesomeric forms ($-CH^{\bullet}-S- \leftrightarrow -CH=S^{\bullet}-$), absorbed at 280 nm in aqueous solution. The formation of the corresponding cation RSR(-H)⁺, as product of disproportionation of the radical RSR(-H)[•], was detected not with absorption measurements (no distinct band was identified on the spectrum), but by conductivity recording.^{4f} The exclusive observation of the cation in our case may be traced back to a different stability of the thionium ions, as supported by a MNDO study performed on this kind of cation.²⁵ In particular, this theoretical treatment has shown that (α -thio)benzyl cation (PhCH⁺SCH₃) is significantly more stable than the corresponding ion with

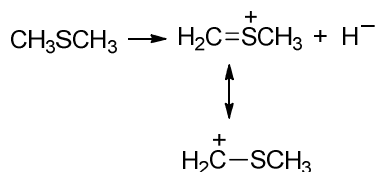
hydrogen in place of phenyl ($\text{CH}_3\text{SCH}_2^+$). The effect of the phenyl substituent on the energetics of thionium ion formation was estimated through $\Delta\Delta\text{H}$ value, namely the difference between the enthalpy change for the reactions shown in Scheme 6 and 7, quantified as -28 kcal/mol. The greater stability of $\text{PhCH}^+\text{SCH}_3$ is due to the fact that its structure can be described in terms of various mesomeric forms (Scheme 6), more numerous than those of $\text{CH}_3\text{SCH}_2^+$ (Scheme 7), as indicated by the values obtained by calculation of the π -bond orders for the two cation structures, equal to 0.60 for CH-S and 0.61 for C-Ph bonds in the benzyl cation, 0.86 for C-S and 0 for C-H bonds in the methylthiomethyl cation.²⁵

Another interesting comparison is with the behavior of the corresponding aromatic thioether cations, PhCH^+SPh , intermediate species whose formation have been invoked in the oxidation of aryl benzyl sulfides studied by pulse radiolysis and laser flash photolysis, but never experimentally observed.^{3d,e,h} This different behavior could be explained on the basis of the lower stability of PhCH^+SPh with respect to $\text{PhCH}^+\text{SCH}_3$, as the feasible conjugation between the sulfur atom and the near aromatic π system could prevent an efficient intervention of the sulfur to the delocalization of the positive charge.

Scheme 6



Scheme 7



Another interesting observation is that the (α -thiomethyl)benzyl radical, to be oxidized by the ground state sensitizer (see Scheme 4), should have an oxidation potential more negative than that of MeOP⁺ (-0.81 V vs SCE in MeCN, obtained from the corresponding N-ethyl structure)^{7b} and this is in agreement with a very stable (α -thiomethyl)benzyl cation.²⁶ The oxidation potentials of similar radicals, such as C₆H₅-CH[•]OCH₃ and C₆H₅-CH[•]OH (-0.33 V and -0.30 V vs SCE in CH₃CN, respectively)^{28,29} point out a significant lower stability of the corresponding cations and would not make oxidation practicable.

From the decay kinetic data of radical cations **1a**^{•+}-**1c**^{•+} reported in Table 2, it can be noted that the deprotonation rates are practically not affected by the substituent type, both in the absence and the presence of the base ($\tau=7\div 8$ and ca. 0.9 μ s, respectively).³⁰ On the contrary, the deprotonation rate constant of toluene radical cation (PhCH₃^{•+}, $k = 1 \times 10^7$ s⁻¹)³¹ in water is nearly five orders of magnitude higher than that of 4-methoxytoluene (4-CH₃O-C₆H₄-CH₃^{•+}, $k = 4 \times 10^2$ s⁻¹)³², taken as a reference. This remarkable dependence on the substituent is explainable considering that 4-CH₃O-C₆H₄-CH₃^{•+} becomes a weaker acid with respect to PhCH₃^{•+} because the methoxy group (an electron-donating substituent) decreases its reduction potential (1.71 V, to compare with 2.35 V of toluene, both vs SCE in CH₃CN).³³ In other words, on the basis of these data it can be stated that for radical cations of such structure the kinetic acidity parallels thermodynamic acidity. In the case of benzyl methyl- and 4-methoxybenzyl methyl sulfide radical cations, the significant amount of spin and positive charge delocalized not only on the ring but also on the sulfur atom (as indicated by DFT calculations), makes weaker the substituent effect. This is reflected by the difference in oxidation potential between **1a** and **1b** (0.08 V, against 0.64 V of the corresponding benzyl derivatives) and then on the kinetic acidity.

Conclusions

Radical cations **1a**^{•+}-**1c**^{•+}, photochemically generated by MeOP⁺, were able to deprotonate and then to form the corresponding aldehyde compounds. Benzyl radicals, namely the intermediates generally observed after the C_α-H bond cleavage, were not sufficiently accumulated to be detected by LFP experiments, but the corresponding (α-thio)benzyl cations (thionium ions) were highlighted, coming from their oxidation. In line with this assignment, the decay rate of these transients (a first order process) were unaffected by oxygen, while their formation reactions were considerably accelerated by the intervention of a base (TBAN). This result has been explained by invoking the stability of the thionium ions, due to a delocalization of the positive charge extended to the whole structure. Until now thionium ions had been pointed out by pulse radiolysis conductivity experiments as intermediates in the oxidation of dialkyl sulfides, but their absorption spectra were never identified.

The lifetimes of the radical cations were very slightly sensitive to the nature of the substituent, both with and without base. These results have been rationalized by considering (DFT calculations) that charge and spin are delocalized among the ring and the sulfur atom, which lead to a resulting leveling of the acid strength of the benzylic position.

Experimental Section

Starting Materials. 4-Methoxybenzyl methyl sulfide (**1a**), benzyl methyl sulfide (**1b**) and 4-trifluoromethylbenzyl methyl sulfide (**1c**) were prepared by reaction of the corresponding benzyl mercaptans with CH₃I in ethyl alcohol according to the procedure described in literature.³⁴ Substrates **1a** and **1b** were characterized as already described.³⁵ The purity of **1c** was checked by NMR and GC-MS analysis. ¹H-NMR (400 MHz, CDCl₃) of **1c**: δ 7.68 (d, 2H), 7.53 (d, 2H), 3.81 (s, 2H), 2.01 (s, 3H). ¹³C NMR (400 MHz, CDCl₃): δ (ppm) 129.2, 128.8, 125.5, 124.2, 37.9; 14.9. GC-MS (70 eV, EI) of **1c**: *m/z* 206 (M⁺, 46), 187 (5), 159 (100), 139 (4), 109 (21), 89 (5), 63 (5). Benzaldehydes **2a-c** and

1
2
3 tetra-*n*-butylammonium nitrate (TBAN) were commercially available. N-Methoxyphenanthridinium
4
5 hexafluorophosphate ($\text{MeOP}^+\text{PF}_6^-$) was prepared according to a literature procedure.^{7a, 36} Acetonitrile
6
7 of HPLC grade for product analysis and acetonitrile of spectrophotometric grade for spectroscopic
8
9 measurements were used as received.
10
11

12 **Steady-State Oxidation.** A solution prepared by dissolving $\text{MeOP}^+\text{PF}_6^-$ (5.0×10^{-3} M) and benzylic
13
14 sulfide (1.0×10^{-2} M) in 10 ml MeCN, was irradiated in an Applied Photophysics multilamp apparatus
15
16 with six phosphor-coated fluorescent lamps (15 W each) emitting at 355 nm ($\Delta\lambda_{1/2} = 20$ nm), at running
17
18 water temperature (15 °C), with argon bubbling through the solution. After irradiation, the reaction
19
20 mixture was analyzed after adding an internal standard (bibenzyl) by GC, GC-MS and ^1H -NMR and
21
22 all products formed were identified by comparison with authentic specimens. The sensitizer analysis
23
24 was performed by optical density measurements on HP-8451 diode array spectrophotometer. The
25
26 material balance was always satisfactory (> 94%).
27
28
29
30
31

32 Blank experiments, performed by keeping a solution of $\text{MeOP}^+\text{PF}_6^-$ and sulfide in the dark or by
33
34 irradiation of solutions in the absence of the sensitizer, showed no formation of products.
35
36

37 **Competitive Experiments** The kinetic experiments were performed at 20 °C by irradiating (as above)
38
39 10 ml of N_2 -saturated CH_3CN solutions containing $\text{MeOP}^+\text{PF}_6^-$ (5.0×10^{-3} M) and the two substrates
40
41 (both 5.0×10^{-3} M). The amounts of the products (benzaldehydes) were determined by GC with respect
42
43 to an internal standard at different times and the values were inserted into a suitable kinetic equation.³⁷
44
45 The reported k_{rel} values are the average of at least three determinations.
46
47
48

49 **Laser Flash Photolysis.** Excitation wavelength of 355 nm (from a Nd:YAG laser, Continuum, third
50
51 harmonic, pulse width ca. 7 ns and energy < 3 mJ per pulse) was used in nanosecond flash photolysis
52
53 experiments.³⁸ The transient spectra were obtained by a point-to-point technique, monitoring the
54
55 change of absorbance (ΔA) after the laser flash at intervals of 5-10 nm over the spectral range 300-800
56
57
58
59
60

nm, averaging at least 10 decays at each wavelength. A 2 ml solution containing the substrate (1.0×10^{-2} M) and the sensitizer ($\text{MeOP}^+\text{PF}_6^-$, 5.0×10^{-3} M) was flashed in a quartz photolysis cell while nitrogen was bubbling through them. The experimental error was $\pm 10\%$.

Cyclic Voltammetry. E_p values were obtained by cyclic voltammetry experiments, conducted with an AMEL 552 potentiostat controlled by a programmable AMEL 568 function generator (cyclic voltammetry at 100 mVs^{-1} , 1mm diameter platinum disc anode and SCE as reference) in CH_3CN – LiClO_4 (0.1 M).

Computational Methodology Quantum mechanical calculations were carried out by using the Gaussian 09 package.¹⁸ Charge and spin density distribution of the radical cations were obtained by using the B3LYP functional, after geometrical optimization performed with the same DFT model. All calculations were performed with a 6-311G(d,p) basis set.³⁹

Acknowledgements. The authors thank MIUR (Ministero dell'Università e della Ricerca, Rome, Italy) and University of Perugia (PRIN 2010–2011, no. 2010FM738P) for funding.

Supporting Information Available: Time-resolved absorption spectra after LFP of the $\text{MeOP}^+/\mathbf{1a}$, $\mathbf{1c}$ systems with and without TBAN, $\text{MeOP}^+/\mathbf{1b}$ system in O_2 -equilibrated CH_3CN and dicumyl peroxide peroxide in the presence of $\mathbf{1b}$; decay kinetics of $\mathbf{1a}^{+\bullet}$ in the presence of TBAN in N_2 - and O_2 -equilibrated CH_3CN ; most stable conformers for $\mathbf{1a}^{+\bullet}$ and $\mathbf{1c}^{+\bullet}$; SOMO of the energy minimum conformers of $\mathbf{1a}^{+\bullet}$ and $\mathbf{1c}^{+\bullet}$; ^1H NMR and ^{13}C NMR spectra of 4-CN- $\text{C}_6\text{H}_4\text{CH}_2\text{SCH}_3$ ($\mathbf{1c}$). This material is available free of charge via the Internet at <http://pubs.acs.org>.

References and notes

1. (a) Bobrowski, K.; Houée-Levin, C.; Marciniak, B. *Chimia* **2008**, *62*, 728-734. (b) Schöneich, C.; Pogocki, D.; Hug, G. L.; Bobrowski, K. *J. Am. Chem. Soc.* **2003**, *125*, 13700-13713. (c) Butterfield, D. A.; Kanski, J. *Peptides* **2002**, *23*, 1299-1309. (d) Schöneich, C. *Arch. Biochem. Biophys.* **2002**, *397*, 370-376. (e) Tobien, T.; Cooper, W. J.; Nickelsen, M. G.; Pernas, E.; O'Shea, K. E.; Asmus, K.-D. *Environ. Sci. Technol.* **2000**, *34*, 1286-1291. (f) Goto, Y.; Matsui, T.; Ozaki, S.; Watanabe, Y.; Fukuzumi, S. *J. Am. Chem. Soc.* **1999**, *121*, 9497-9502. (g) Miller, B. L.; Kuczera, K.; Schöneich, C. *J. Am. Chem. Soc.* **1998**, *120*, 3345-3356. (h) Bobrowski, K.; Hug, G. L.; Marciniak, B.; Miller, B. L.; Schöneich, C. *J. Am. Chem. Soc.* **1997**, *119*, 8000-8011. (i) Baciocchi, E.; Lanzalunga, O.; Pirozzi, B. *Tetrahedron* **1997**, *53*, 12287-12298. (j) Marciniak, B.; Hug, G. L.; Rozwadowski, J.; Bobrowski, K. *J. Am. Chem. Soc.* **1995**, *117*, 127-134. (k) Ozaki, S.; Ortiz de Montellano, P. R. *J. Am. Chem. Soc.* **1995**, *117*, 7056-7064. (l) Kobayashi, S.; Nakano, M.; Kimura, T.; Schaap, A. P. *Biochemistry* **1987**, *26*, 5019-5022.
2. (a) Baciocchi, E.; Bettoni, M.; Del Giacco, T.; Lanzalunga, O.; Mazzonna, M.; Mencarelli, P. *J. Org. Chem.* **2011**, *76*, 573-582. (b) Del Giacco, T.; Lanzalunga, O.; Mazzonna, M.; Mencarelli, P. *J. Org. Chem.* **2012**, *77*, 1843-1852. (c) Baciocchi, E.; Del Giacco, T.; Gerini, M. F.; Lanzalunga, O. *Org. Lett.* **2006**, *8*, 641-644. (d) Filipiak, P.; Hug, G.L.; Bobrowski, K.; Marciniak, B. *J. Photochem. Photobiol. A Chem.* **2006**, *177*, 295-306. (e) Memarian H. R.; Baltork I. M.; Bahrani K. *Bull. Korean Chem. Soc.* **2006**, *27*, 106-110. (f) Latour, V.; Pigot, T.; Simon, M.; Cardy H.; Lacombe, S. *Photochem. Photobiol. Sci.* **2005**, *4*, 221-229. (g) Filipiak, P.; Hug, G.L.; Carmichael, I.; Korzeniowska-Sobczuk, A.; Bobrowski, K.; Marciniak, B. *J. Phys. Chem. A* **2004**, *108*, 6503-6512. (h) Baciocchi, E.; Del Giacco, T.; Elisei, F.; Gerini, M. F.; Guerra, M.; Lapi, A.; Liberali, P. *J. Am. Chem. Soc.* **2003**, *125*, 16444-16454.

3. (a) Lanzalunga, O.; Lapi, A. *J. Sulfur Chem.* **2012**, *23*, 101-129. (b) Peñeñory, A. B.; Argüello, J. E.; Puiatti, M. *Eur. J. Org. Chem.* **2005**, *1*, 114-122. (c) Baciocchi, E.; Gerini, M. F.; Lanzalunga, O.; Lapi, A.; Lo Piparo, M. G. *Org. Biomol. Chem.* **2003**, *1*, 422-426. (d) Del Giacco, T.; Elisei, F.; Lanzaunga O. *Phys. Chem. Chem. Phys.* **2000**, *2*, 1701-1708. (e) Baciocchi, E.; Lanzaunga, O.; Malandruccho, S.; Ioele, M.; Steenken, S. *J. Am. Chem. Soc.* **1996**, *118*, 8973-8974. (f) Baciocchi, E.; Crescenzi, C.; Lanzaunga, O. *Tetrahedron* **1997**, *53*, 4469-4478. (g) Baciocchi, E.; Del Giacco T.; Ferrero, M. I.; Rol, C.; Sebastiani, G. V. *J. Org. Chem.* **1997**, *62*, 4015-4017. (h) Ioele, M.; Steenken, S.; Baciocchi, E. *J. Phys. Chem. A* **1997**, *101*, 2979-2987.
4. (a) Chaudhri, S. A.; Mohan, H.; Anklam, E.; Asmus, K.-D. *J. Chem. Soc., Perkin Trans. 2*, **1996**, 383-390. (b) Goebel, M.; Bonifacic, M.; Asmus, K.-D. *J. Am. Chem. Soc.* **1984**, *106*, 5984-5988. (c) Chaudhri, S. A.; Goebel, M.; Freyholdt, T.; Asmus, K.-D. *J. Am. Chem. Soc.* **1984**, *106*, 5988-5992. (d) Asmus, K.-D. *Acc. Chem. Res.* **1979**, *12*, 436-442. (e) Asmus, K.-D.; Bahnemann, D.; Fischer, C. H.; Veltwisch, D. *J. Am. Chem. Soc.* **1979**, *101*, 5322-5329. (f) Bonifačić, M.; Möckel, H.; Bahnemann D.; Asmus, K.-D. *J. Chem. Soc., Perkin Trans 2*, **1975**, 675-685.
5. Yokoi, H.; Hatta, A.; Ishiguro, K.; Sawaki, Y. *J. Am. Chem. Soc.* **1998**, *120*, 12728-12733.
6. (a) Baciocchi, E.; Del Giacco, T.; Elisei, F.; Lapi A. *J. Org. Chem.* **2006**, *71*, 853-860. (b) Baciocchi, E.; Del Giacco, T.; Elisei, F.; Gerini, M. F.; Lapi, A.; Liberali, P.; Uzzoli, B. *J. Org. Chem.* **2004**, *69*, 8323-8330.
7. (a) Shukla, D.; Liu, G.; Dinnocenzo, J. P.; Farid, S. *Can. J. Chem.* **2003**, *81*, 744-757. (b) Wosinska, Z. M.; Stump, F. L.; Ranjan, R.; Lorange, E. D.; Finley, G. N.; Patel, P. P.; Khawaja, M. A.; Odom, K. L.; Kramer, W. H.; Gould, I. R. *Photochemistry and Photobiology* **2014**, *90*, 313-328.
8. Only for **1c**, traces (< 1%) of 1,2-(4-cyanophenyl)-1,2-bis(methylthio)ethane, [4-CN-C₆H₄CH(SCH₃)₂], were detected together with 4-CF₃-C₆H₄CHO.
9. Bonesi, S. M.; Fagnoni, M.; Albini, A. *Eur. J. Org. Chem.* **2008**, *15*, 2612-2620.

10. Julliard M. In *Photoinduced Electron Transfer*, Part B; Fox, M. A and Chanon M., Eds.; Elsevier: Amsterdam, 1988; Chapter 2.5.
11. Chaudhri, S. A.; Gobl, M.; Freyholdt, T.; Asmus, K.-D. *J. Am. Chem. Soc.* **1984**, *106*, 5988-5992.
12. Filipiak, P.; Hug, G. L.; Carmichael, I.; Korzeniowska-Sobczuk, A.; Bobrowski, K.; Marciniak, B. *J. Phys. Chem. A* **2004**, *108*, 6503-6512.
13. Avila, D. V.; Ingold, K. U.; Di Nardo, A. A.; Zerbetto, F.; Zgierski, M. Z.; Luszyk, J. *J. Am. Chem. Soc.* **1995**, *117*, 2711-2718.
14. Likewise DFT calculations indicate the radical $\text{C}_6\text{H}_5\text{CH}^\bullet\text{SCH}_2\text{COO}^-$ to absorb mainly at 335 nm in the gas phase.¹² The substituent on the ring is expected to have little influence on the radical absorption. Indeed, the corresponding radicals $(4\text{X-C}_6\text{H}_5)_2\text{CH}^\bullet$, having an aryl in place of the thiomethyl group, absorb at 350, 330 and 334 nm with X = OCH₃, H and CF₃, respectively.¹⁵
15. Bartl, J.; Steenken, S.; Mayr, H.; McClelland, R. A. *J. Am. Chem. Soc.* **1990**, *112*, 6918-6928.
16. For example, cations such as $(4\text{X-C}_6\text{H}_5)_2\text{CH}^+$ absorb at $\lambda_{\text{max}} = 500, 435$ and 425 nm, while the corresponding radicals $(4\text{X-C}_6\text{H}_5)_2\text{CH}^\bullet$, absorb at 350, 330 and 334 nm with X = OCH₃, H and CF₃, respectively.¹⁵
17. In more anhydrous MeCN, the cation turned out to decay with a longer lifetime.
18. Frisch, M. J.; Trucks, G. W.; Schlegel, H. B.; Scuseria, G. E.; Robb, M. A.; Cheeseman, J. R.; Scalmani, G.; Barone, V.; Mennucci, B.; Petersson, G. A.; Nakatsuji, H.; Caricato, M.; Li, X.; Hratchian, H. P.; Izmaylov, A. F.; Bloino, J.; Zheng, G.; Sonnenberg, J. L.; Hada, M.; Ehara, M.; Toyota, K.; Fukuda, R.; Hasegawa, J.; Ishida, M.; Nakajima, T.; Honda, Y.; Kitao, O.; Nakai, H.; Vreven, T.; Montgomery Jr., J. A.; Peralta, J. E.; Ogliaro, F.; Bearpark, M.; Heyd, J. J.; Brothers, E.; Kudin, K. N.; Staroverov, V. N.; Keith, T.; Kobayashi, R.; Normand, J.; Raghavachari, K.; Rendell, A.; Burant, J. C.; Iyengar, S. S.; Tomasi, J.; Cossi, M.; Rega, N.; Millam, J. M.; Klene, M.; Knox, J. E.; Cross, J. B.; Bakken, V.; Adamo, C.; Jaramillo, J.; Gomperts, R.; Stratmann, R. E.;

Yazyev, O.; Austin, A. J.; Cammi, R.; Pomelli, C.; Ochterski, J. W.; Martin, R. L.; Morokuma, K.; Zakrzewski, V. G.; Voth, G. A.; Salvador, P.; Dannenberg, J. J.; Dapprich, S.; Daniels, A. D.; Farkas, O.; Foresman, J. B.; Ortiz, J. V.; Cioslowski, J.; Fox, D. J. GAUSSIAN 09 (Revision B.01), Gaussian, Inc., Wallingford, CT, 2010.

19. Indeed, the oxidation potential value of 4-methoxybenzyl methyl sulfide (1.55 V, Table 1) is close enough to that of 4-methoxytoluene (1.71 V)²⁰, a structure for which charge and spin in the corresponding radical cation can be exclusively on the aromatic ring. On the contrary, benzyl methyl sulfide oxidation potential (1.63 V) is somewhat lower than that of the corresponding toluene (2.35 V)²¹, in agreement with a greater contribution of structure I to the radical cation structure when the stabilizing effect of the substituent is missing.
20. Fukuzumi S.; Kochi, J.K. *J. Am. Chem. Soc.* **1981**, *103*, 7240-7252.
21. Dockery, K. P.; Dinnocenzo, J. P.; Farid, S.; Goodman, J. L.; Gould, R.; Todd, W. P. *J. Am. Chem. Soc.* **1997**, *119*, 1876–1883.
22. Baciocchi, E.; Rol, C.; Scamosci, E.; Sebastiani, G.V. *J. Org. Chem.* **1991**, *56*, 5498-5502.
23. The bond dissociation free energy of the C_α-S cleavage in the PhCH₂SCH₂CH₃^{•+} (BDFE of 28 kcal/mol) was estimated to be much more endergonic than the C_α-H bond fragmentation reaction (BDFE of -8 kcal/mol). The breaking of the two bonds in the aromatic sulfide radical cations is instead characterized by similar ΔH° values.²⁴
24. Baciocchi, E. *Acta Chem. Scand.* **1990**, *44*, 645-652.
25. Ginsburg, J. L.; Langler, R. F. *Can. J. Chem.* **1983**, *61*, 589-593.
26. On the other hand, Albini et al. suggested the oxidation of the analogous radical PhCH[•]SCH₂CH₃ by the ground state of DCA,⁹ although the sensitizer potential is even more negative (-0.89 V vs.SCE in MeCN)²⁷ than that of MeOP⁺.
27. Breslin, D. T.; Fox, M. A. *J. Am. Chem. Soc.* **1993**, *115*, 11716-11721.

28. Lund, V T.; Wayner, D. D. M.; Jonsson, M.; Larsen, A. G.; Daasbjerg, K. *J. Am. Chem. Soc.* **2001**, *123*, 12590–12595.
29. Wayner, D. D.; Houmam, A. *Acta Chem. Scand.* **1998**, *52*, 377-384.
30. Since the relative rate does not vary in the presence of the base, it can be assumed that the radical cation decay rate matches with the deprotonation rate; hence this reaction is the rate-determining step, in line with the limited accumulation of this intermediate.
31. Sehested, K.; Holcman, J. *J. Phys. Chem.* **1978**, *82*, 651–653.
32. Baciocchi, E.; Bietti, M.; Manduchi, L.; Steenken, S. *J. Am. Chem. Soc.* **1999**, *121*, 6624–6629.
33. Baciocchi, E.; Bietti, M.; Lanzalunga, O. *J. Phys. Org. Chem.* **2006**, *19*, 467–478.
34. Labuschagne, A. J. H.; Malherbe, J. S.; Meyer, C. J.; Schneider, D. F. *J. Chem. Soc., Perkin Trans. I* **1978**, 955-961.
35. (a) Van Est-Stammer, R.; Engberts, J. B. F. N. *Can. J. Chem.* **1973**, *51*, 1187-1192. (b) Adcock, I. W.; Gupta, B. D. *J. Org. Chem.* **1976**, *41*, 1498-1504. (c) Zairaiskii, A. P.; Kachurin, O. I. *Russ. J. Org. Chem.* **2003**, *39*, 1642-1645. (d) Holland, H. L.; Brown, F. M.; Kerridge, A.; Turner, C. D. *J. Mol. Cat. B: Enzymatic* **1999**, *6*, 463–471. (d) Holland, H. L.; Brown, F. M.; Kerridge, A.; Turner, C. D. *J. Mol. Cat. B: Enzymatic* **1999**, *6*, 463–471.
36. Lorange, E. D.; Kramer, W. H.; Gould, I. R. *J. Am. Chem. Soc.* **2002**, *124*, 15225–15238.
37. Bunnett, J. F. In *Investigation of Rates and Mechanism of Reactions*; ed. E. S. Lewis, Wiley, New York, 1974; part I, pp. 158-161.
38. Görner, H.; Elisei, F.; Aloisi, G. G. *J. Chem. Soc., Faraday Trans.* **1992**, *88*, 29-34.
39. Masunov, A. M.; Tretiak, S. *J. Phys. Chem. B* **2004**, *108*, 899–907.